PIBB 生物化学与生物物理进展
Progress in Biochemistry and Biophysics
2024, 51(10): 2730~2740
www.pibb.ac.cn

Engineering The Neck Hinge Reshapes The Processive Movement of Kinesin-3*

LI Dong[1,3)**], REN Jin-Qi[1)**], SONG Yin-Long[2)], LIANG Xin[2)***], FENG Wei[1,3)***]

([1)]*Key Laboratory of Biomacromolecules (CAS), National Laboratory of Biomacromolecules, CAS Center for Excellence in Biomacromolecules, Institute of Biophysics, Chinese Academy of Sciences, Beijing* 100101, China;
[2)]*School of Life Sciences, Tsinghua University, Beijing* 100084, China;
[3)]*College of Life Sciences, University of Chinese Academy of Sciences, Beijing* 100049, China)

Abstract **Objective** In kinesin-3, the neck coil correlates with the following segments to form an extended neck that contains a characteristic hinge diverse from a proline in KIF13B to a long flexible linker in KIF1A. The function of this neck hinge for controlling processive movement, however, remains unclear. **Methods** We made a series of modifications to the neck hinges of KIF13B and KIF1A and tested their movement using a single-molecule motility assay. **Results** In KIF13B, the insertion of flexible residues before or after the proline differentially impacts the processivity or velocity, while the removal of this proline increases the both. In KIF1A, the deletion of entire flexible neck hinge merely enhances the processivity. The engineering of these hinge-truncated necks of kinesin-3 into kinesin-1 similarly boosts the processive movement of kinesin-1. **Conclusion** The neck hinge in kinesin-3 controls its processive movement and proper modifications tune the motor motility, which provides a novel strategy to reshape the processive movement of kinesin motors.

Key words intracellular transport, molecular motor, kinesin-3, neck hinge, processive movement
DOI: 10.16476/j.pibb.2024.0269

Kinesins are microtubule-based molecular motors critical for intracellular transport and microtubule network organization[1-3]. Kinesin motors feature a motor domain (MD) that binds to microtubules and nucleotides, converting the chemical energy of ATP hydrolysis into mechanical force[4-5]. For effective movement along microtubule tracks, processive kinesins (kinesin-1/2/3) require not only the MD but also a neighboring neck domain, comprising a neck linker (NL) and a neck coil (NC) [4, 6]. The NC forms a coiled-coil dimer, brings two MDs together to assemble a "two-headed" motor. Meanwhile, the NL, in coordination with the nucleotide exchange of the MD, docks or undocks from the MD to control directionality[7-9]. Based on the NC-mediated motor dimer, the length of the NL determines the inter-head strain between the two MDs, which is essential for controlling velocity and processivity[10-11]. Moreover, the biophysical property and stability of the NC coiled-coil dimer further modulate the processivity[12-13]. Thus, the entire neck domain, along with the motor domain, orchestrates kinesin motors' processive movement. Defining the mechanical and biochemical factors that determine kinesin processivity is crucial for understanding how various kinesins are optimized for specific cellular functions.

Kinesin-3, a subfamily of kinesins comprises diverse members including KIF1A/B/C, KIF13A/B,

* This work was supported by grants from the Beijing Natural Science Foundation (5242021), the Strategic Priority Research Program of CAS (XDB37020302), The National Natural Science Foundation of China (32071191, 32371273), the Chinese National Programs for Brain Science and Brain-like Intelligence Technology (2022ZD0205800), and the CAS Project for Young Scientists in Basic Research (075).
** These authors contributed equally to this work.
*** Corresponding author.
LIANG Xin. Tel: 86-10-62771231, E-mail: xinliang@mail.tsinghua.edu.cn
FENG Wei. Tel: 86-10-64888751, E-mail: wfeng@ibp.ac.cn
Received: June 26, 2024 Accepted: August 24, 2024

and KIF16A/B[2, 4]. The processivity of kinesin-3, which is 10 times greater than that of kinesin-1, fine-tunes it for long-distance intracellular transport[14]. In addition to the motor and neck domains, kinesin-3 contains a family-specific forkhead-associated (FHA) domain flanked by two coiled-coils (CC1 and CC2) (Figure S1a), distinguishing it from conventional kinesin-1. Both KIF1A and KIF13B contain an MBS (MAGUK binding stalk)-MATH (meprin and TRAF-C homology) tandem and a large undefined region (UDR) that follow CC2 (Figure S1a). The MBS-MATH tandem is involved in kinesin auto-inhibition[15], while the precise function of UDR is unknown. The C-terminal PH (Pleckstrin homology) domain of KIF1A is responsible for cargo binding while the C-terminal CAP-Gly (cytoskeleton-associated protein-glycine-rich) of KIF13B can control motor landing and processivity by influencing the initial motor-microtubule interaction[16-17]. For kinesin-3, the NC, CC1, and FHA can form a central hub for controlling motor activity[18]. In comparison to conventional kinesin-1, the NC of kinesin-3 is relatively shorter and tends to form an unstable coiled-coil dimer that can be inhibited by CC1 for autoinhibition[14, 19]. In the inhibited state, CC1 is broken into several short helices that fold back to associate with both the NC and MD and lock down the entire neck domain by blocking the NC dimer formation and the NL undocking from the MD[15, 20]. On the other hand, the FHA domain can work with CC1 to form a stable CC1-FHA dimer that releases the CC1-mediated inhibition and promotes the NC dimer formation[18, 21]. Thus, in the uninhibited state, the NC tends to coordinate with the CC1-FHA tandem to form a stable dimeric neck for processive movement, and the neck domain of kinesin-3 could be extended to the FHA domain (*i.e.*, the NC-CC1-FHA tandem)[21].

In the NC-CC1-FHA tandem, the NC, CC1, and the FHA domain are highly conserved among the different members of kinesin-3, but the hinge between the NC and CC1 (referred to as the neck hinge) is diverse in length and flexibility, *e.g.*, from a proline in KIF13A/B to a long flexible linker in KIF1A/B/C (Figure S1b). The function of this diverse neck hinge in the extended neck domain of kinesin-3 for controlling processive movement remains unclear. In this study, we make a number of mutations in the neck hinges of KIF13B and KIF1A. In KIF13B, the insertion of flexible residues before or after the proline differentially impacts the processivity or velocity, while the deletion of this proline increases both. In KIF1A, the truncation of the flexible neck hinge affects the processivity. The engineering of these mutated neck domains into kinesin-1 also boosts the processive movement of kinesin-1. Thus, the neck hinge in kinesin-3 can be modified to tune its processive movement.

1 Materials and methods

1.1 Protein expression and purification

The plasmid for *Drosophila melanogaster* kinesin heavy chain (*Dm*KHCΔ521-642) (referred to as KHC) was a gift of Dr. Vladimir I. Gelfand (Northwestern University, Chicago, USA). DNA sequences encoding the KHC-KIF1A ΔHinge and KHC-KIF13B ΔP391 chimeras (with the MD and NL from KHC) were each cloned into a modified version of the pET32a vector. DNA sequences encoding mouse KIF13B fragments including the MD-NC tandem (residues 1−389), the MD-NC-CC1 tandem (residues 1−432), and the MD-NC-CC1-FHA tandem (residues 1−546) and that encoding the MD-NC-CC1-FHA tandem (residues 1−613) of mouse KIF1A were also each cloned into a modified version of the pET32a vector. All the mutations in the KIF13B and KIF1A fragments were created using the standard PCR-based mutagenesis method and confirmed by DNA sequencing. Recombinant proteins were expressed in *Escherichia coli* BL21 (codon plus) host cells at 16°C. After the 16 h cultivation, the cells were harvested and suspended in the buffer containing 50 mmol/L Tris-HCl, pH7.5, 500 mmol/L $(NH_4)_2SO_4$, 2 mmol/L $MgCl_2$, 1 mmol/L EGTA, 1 mmol/L PMSF, 0.5 mmol/L ATP. The proteins were purified by Ni^{2+}-Sepharose 6 Fast Flow (GE Healthcare) affinity chromatography with the washing buffer (50 mmol/L Tris-HCl, pH7.5, 500 mmol/L $(NH_4)_2SO_4$, 2 mmol/L $MgCl_2$, 1 mmol/L EGTA, 0.1 mmol/L ATP, 40 mmol/L imidazole) and the elution buffer (50 mmol/L Tris-HCl, pH7.5, 500 mmol/L $(NH_4)_2SO_4$, 2 mmol/L $MgCl_2$, 1 mmol/L EGTA, 0.1 mmol/L ATP, 500 mmol/L imidazole). The proteins were further purified by size-exclusion chromatography (Superdex-200 26/60, GE Healthcare) with the buffer containing 150 mmol/L NaCl, 50 mmol/L Tris-HCl, pH7.5, 2 mmol/L $MgCl_2$, 1 mmol/L EGTA, 0.1 mmol/L ATP, and 1 mmol/L

DTT.

1.2 Tubulin purification and labeling

Crude tubulins were obtained from porcine brain through double cycles of polymerization and depolymerization, as previously described[22]. Tubulins were further purified using a TOG-based affinity column[23]. Tubulins were labeled with 5-carboxytetramethylrhodamine (TAMRA, Thermo Fisher Scientific) using NHS esters, following standard protocols[24].

1.3 Polymerization of taxol−stabilized microtubules

A previously published protocol was followed for the *in vitro* motility assay[25]. Briefly, short microtubule seeds were prepared by incubating 32 μmol/L porcine brain tubulin mixture containing 5% TAMRA-labeled tubulin with 1 mmol/L GTP, 4 mmol/L $MgCl_2$, and 4% DMSO. After incubation on ice for 5 min, the mixture was polymerized in a 37°C water bath overnight in the dark. Then, 400 μl of the warm BRB80 buffer (80 mmol/L PIPES/KOH, pH6.9, 1 mmol/L $MgCl_2$, 1 mmol/L EGTA) containing 20 μmol/L taxol was added to stop the reaction. The sample was subjected to centrifugation at 15 000*g* for 20 min at 25° C to collect microtubule seeds in the 200 μl prewarmed taxol-BRB80 buffer.

1.4 Single molecule assay by total internal reflection fluorescence microscopy

Imaging was performed using a total internal reflection (TIRF) microscope (Olympus) equipped with an Andor 897 Ultra EMCCD camera (Andor, Belfast, UK) using a 100× TIRF objective (NA 1.49, Olympus). Polymerized microtubules were diluted in the taxol-BRB80 buffer and then flowed into a flow cell and incubated for 10 min at room temperature to adsorb onto the coverslip surface coated with anti-tubulin antibodies (Sigma). Subsequently, polymerized microtubules were protected from laser illumination by flowing the basic reaction mix buffer (RM) (0.08 g/L glucose oxidase, 0.032 g/L catalase, 0.16 g/L casein, 1% β-mercaptoethanol, 0.001% tween 20, 1 mmol/L $MgCl_2$, 20 μmol/L taxol, 80 mmol/L D-glucose). Finally, a 50 μl final reaction mix consisting of kinesin motors, RM, and 2 mmol/L ATP was added to the flow chamber and the time-lapse movies were recorded. Images were taken every 0.1 s with a 0.05 s exposure at low laser power to avoid photo-bleaching during processive motor runs.

1.5 Data analysis

In order to screen out the single-molecule in the motility assay, we counted the fluorescence intensities of all the moving molecules and carried out the multi-peak Gaussian fitting of their fluorescence intensity distributions. The peak fitted with the minimum value was chosen as the fluorescence intensity distribution of the single molecule, and based on the value and half-height width of the fitted peak, the fluorescence intensity range of the single molecule was estimated. With the multi-peak Gaussian fitting, the fluorescence intensity of a single MNCF-GFP dimer was estimated to be 632±163 (a.u.), and by using this standard, the single molecule was selected and the velocity and run length of the single molecule were calculated.

In the single molecule motility assay, the position of fluorescent motor spots was manually tracked using the ImageJ software (Fiji, NIH) [26]. In the kymograph, the vertical distance represented the time and the horizontal distance indicated the run length. The ratio between the run length and the time was the velocity. The number of events for each protein sample was plotted for the velocity and run length as a histogram and fitted to a Gaussian distribution. All the statistical analyses were performed using GraphPad Prism (GraphPad Software), and all the data were presented as mean±SD. All the *P* values were calculated by using a two-tailed unpaired Student *t* test.

2 Results

2.1 Processive movement of kinesin−3 with an extended neck

We previously demonstrated that the CC1-FHA tandem in kinesin-3 forms a stable dimer that releases the CC1-mediated inhibition and coordinates with the NC to assemble an extended dimeric neck[18, 21]. To evaluate whether this extended neck is essential for processive movement, we initiated this work with the biochemical characterization of the locomotory capacities of different KIF13B fragments (including the MD and the NC-CC1-FHA tandem with a C-terminal GFP tag) by the total internal reflection fluorescence (TIRF) -based single molecule motility assay (Figure S1c, S2a). As expected, the MD-NC and MD-NC-CC1 fragments could bind to microtubules but exhibited no obvious motilities, while the MD-NC-CC1-FHA fragment moved along microtubules

processively (Figure S2b), suggesting that the inclusion of the FHA domain is essential for the processive movement of KIF13B. Thus, the minimal fragment of KIF13B for processive movement is the MD-NC-CC1-FHA fragment. Consistently, the MD-NC-CC1-FHA fragment of KIF1A possessed similar motility with obvious processive movement on microtubule tracks (Figure S2a, b), supporting the locomotory capacity of the kinesin-3 fragment with an extended neck. Based on the motility assay, the MD-NC-CC1-FHA fragments of KIF13B and KIF1A with an extended neck (referred to as the MNCF fragment) were chosen for further characterization of the neck hinge.

2.2 Breakage of the proline−hinge impacts the processive movement of KIF13B

In KIF13A/B, the neck hinge between the NC and CC1 only contains a proline that forms a sharp turn to connect the two coiled-coil segments for structural correlation[21]. To investigate the potential role of this proline-hinge for processive movement, we inserted a number of flexible residues (the $(Gly\text{-}Ser)_3$-linker) before or after this proline (*i.e.*, the $_3$(GS)-P and P-$_3$(GS) mutations) to loosen the sharp turn between the NC and CC1 in the extended neck (Figure 1a). In comparison to the wild-type MNCF fragment of KIF13B, the two different types of insertions unexpectedly have distinct impacts on the processive movement of KIF13B (Figure 1b, c). The $_3$(GS)-P mutation significantly increased the run length (from (2.76±0.43) μm to (7.32±0.69) μm) but slightly enhanced the speed (from (1.54±0.02) μm/s to (1.72±0.02) μm/s) (Figure 1c, d). In contrast, the P-$_3$(GS) mutation enhanced the speed obviously (from (1.54±0.02) μm/s to (2.61±0.08) μm/s) but not the run length (Figure 1c, d). Thus, the different modes of the proline-hinge breakage in KIF13B specifically modulate the processivity and velocity.

Based on the established mechanism for the processive movement of transport kinesins, the mechanical stability of the NC coiled-coil dimer can control the run length (*i.e.*, the dissociation of the NC dimer would pause processive movement) [13, 27-28]. Moreover, given that kinesin motors often asymmetrically walk along microtubules in a hand-over-hand manner[29-31], the continuous movement would generate certain torsion force that could be buffered and stored in the neck domain for controlling the speed[32-34]. Accordingly, the intrinsic flexibility of the neck domain is also of functional importance for controlling motor motility[35-37].

The striking impacts of the different proline-hinge breakages on the processivity and velocity demonstrated the essential role of this proline-hinge in restricting the processive movement of KIF13B (Figure 1c, d). Previous structural studies of the NC-CC1-FHA tandem demonstrated that the proline-hinge adopts a sharp turn between the NC and CC1 and seems to act as a tight joint to connect the two coiled-coil segments[21]. This sharp turn somewhat bends the C-terminal end of the NC and tends to disfavor the coiled-coil dimer formation (Figure S3a), which would restrain the run length. The insertion of flexible residues before the proline would extend the C-terminal end of the NC and stabilize the coiled-coil dimer (Figure S3a), which would release the restrain and increase the run length of the motor. On the other hand, the insertion of flexible residues after the proline would not significantly impact the stability of the NC coiled-coil dimer but provide the additional flexibility between the NC and CC1 (Figure S3a), which would facilitate the storage of potential torsions (generated by the asymmetric walking) for enhancing the motor speed. Consistently, the extra flexibility in the neck domain provided by the insertion of flexible residues before the proline also slightly increased the velocity (Figure 1c, d). Nevertheless, the molecular basis for the striking impacts of the different proline-hinge breakages on the processive movement of KIF13B awaits further investigations.

2.3 Removal of the proline−hinge enhances the motility of KIF13B

Since the proline-hinge restricts processive movement, we removed this proline-hinge from the extended neck of KIF13B (the ΔP391 mutation) (Figure 1a). As expected, in comparison to the wild-type fragment, the ΔP391 mutation significantly enchanted both the run length (from (2.76±0.43) μm to (7.74±0.68) μm) and speed (from (1.54±0.02) μm/s to (2.21±0.01) μm/s) (Figure 1b−d), consistent with the previous studies of this deletion mutation[14]. Our structural studies of the proline-hinge-deletion mutant demonstrated that, after the removal of the proline, the NC and CC1 unexpectedly form a continuous coiled-coil dimer in the NC-CC1-FHA tandem and function together as an extended dimeric neck for controlling

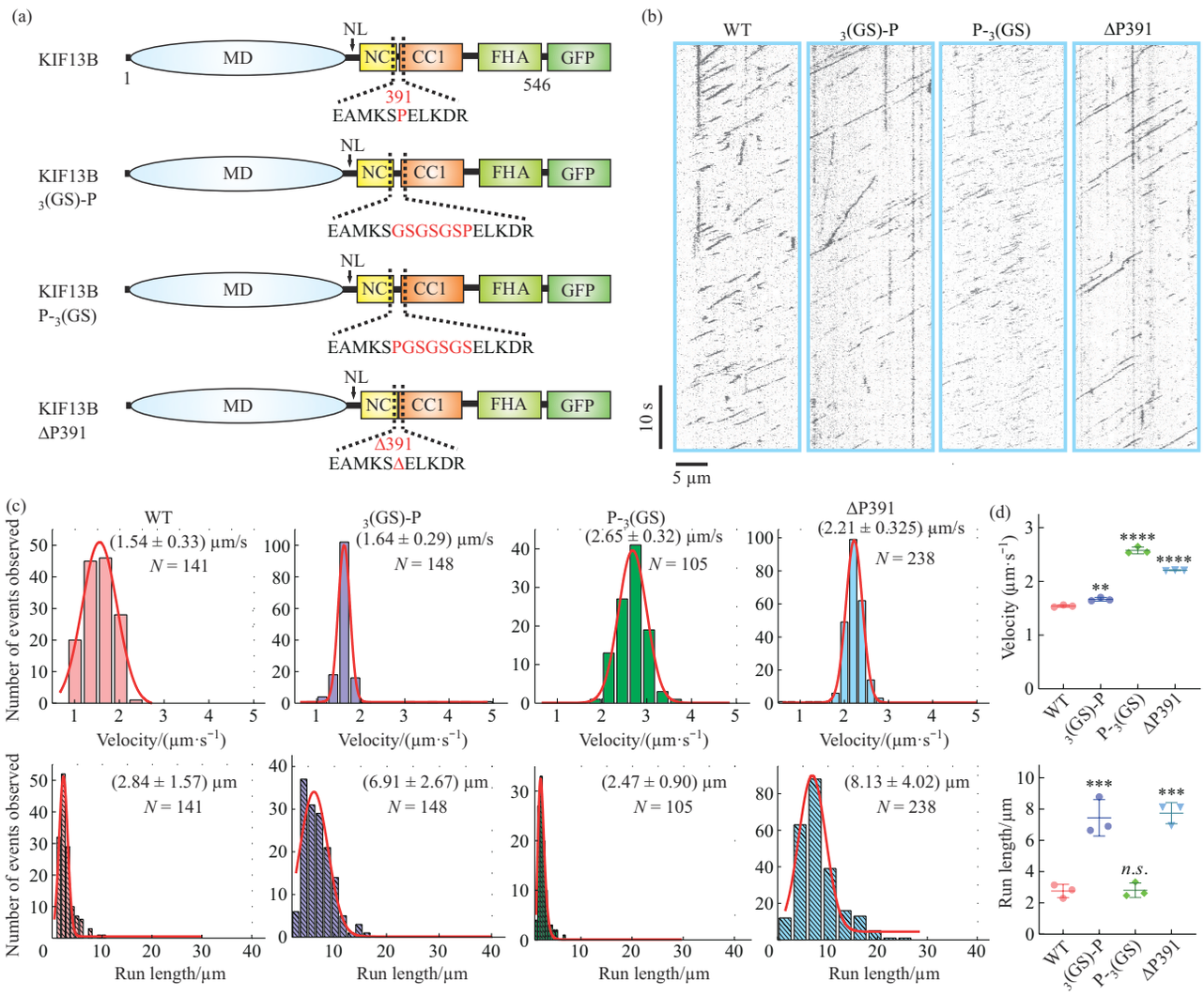

Fig. 1　Mutations of the proline−hinge impact the processive movement of KIF13B

(a) Domain organizations of the MNCF fragment of KIF13B and its various mutants ($_3$(GS)-P, P-$_3$(GS) and ΔP391) used for the single molecule motility assay. (b) Representative kymographs showing the motions of the wild-type (WT) MNCF fragment of KIF13B and the $_3$(GS)-P, P-$_3$(GS) and ΔP391 mutants along microtubules. (c) Quantifications of the velocity (top) and run length (bottom) for each protein sample. The number of events for each protein sample is plotted for the velocity and run length as a histogram and fitted to a Gaussian distribution. The velocity and run length of the corresponding population of the protein sample (*N*) are indicated in each panel as mean±SD. All the data are the average from at least two independent experiments. (d) Statistical analyses of the velocity (top) and run length (bottom) for each protein sample. Statistical significance for the velocity or run length is determined using Student's *t* test (*n.s.*, statistically not significant; ***P*< 0.01; ****P*<0.001; *****P*<0.000 1) as compared with the WT fragment of KIF13B.

processive movement[21] (Figure S3a). This extended continuous coiled-coil dimer would be more stable and also exhibit more capacities of storing the potential torsions (Figure S3a), which would increase both the run length and speed of the motor. Taken together, in the wild-type protein, the proline-hinge in the extended neck of KIF13B restrains processive movement and the motor is somewhat adapted to move with the compromised motility for specific cellular functions. The breakage or removal of this proline-hinge significantly impacts processive movement, demonstrating that the modifications of the neck hinge in KIF13B can tune its processive movement.

2.4　Deletion of the flexible neck hinge increases the processivity of KIF1A

The positive impacts of the neck hinge modifications on the processive movement of KIF13B encouraged us to further investigate the flexible neck hinge in KIF1A (Figure S1b). Since the neck hinge in KIF1A is much longer than that in KIF13B, we

deleted this flexible neck hinge from the MNCF fragment of KIF1A (the ΔHinge mutation) (Figure 2a). Unexpectedly, in comparison to the wild-type fragment, the ΔHinge mutation significantly increased the run length (from (6.39±0.22) μm to (16.44±2.53) μm) but not the speed (Figure 2b−d). To check whether the proline-hinge in KIF13B has a similar restriction effect in KIF1A, we further made the reversal insertion of the proline into the ΔHinge mutant (the ΔHinge-P mutation) (Figure 2a). However, the proline-hinge insertion had no further effects on the motor motility with the similar run length and speed ((16.44±2.53) μm *v. s.* (15.39±0.92) μm, (3.48±0.02) μm/s *v. s.* (3.38±0.03) μm/s) (Figure 2b−d).

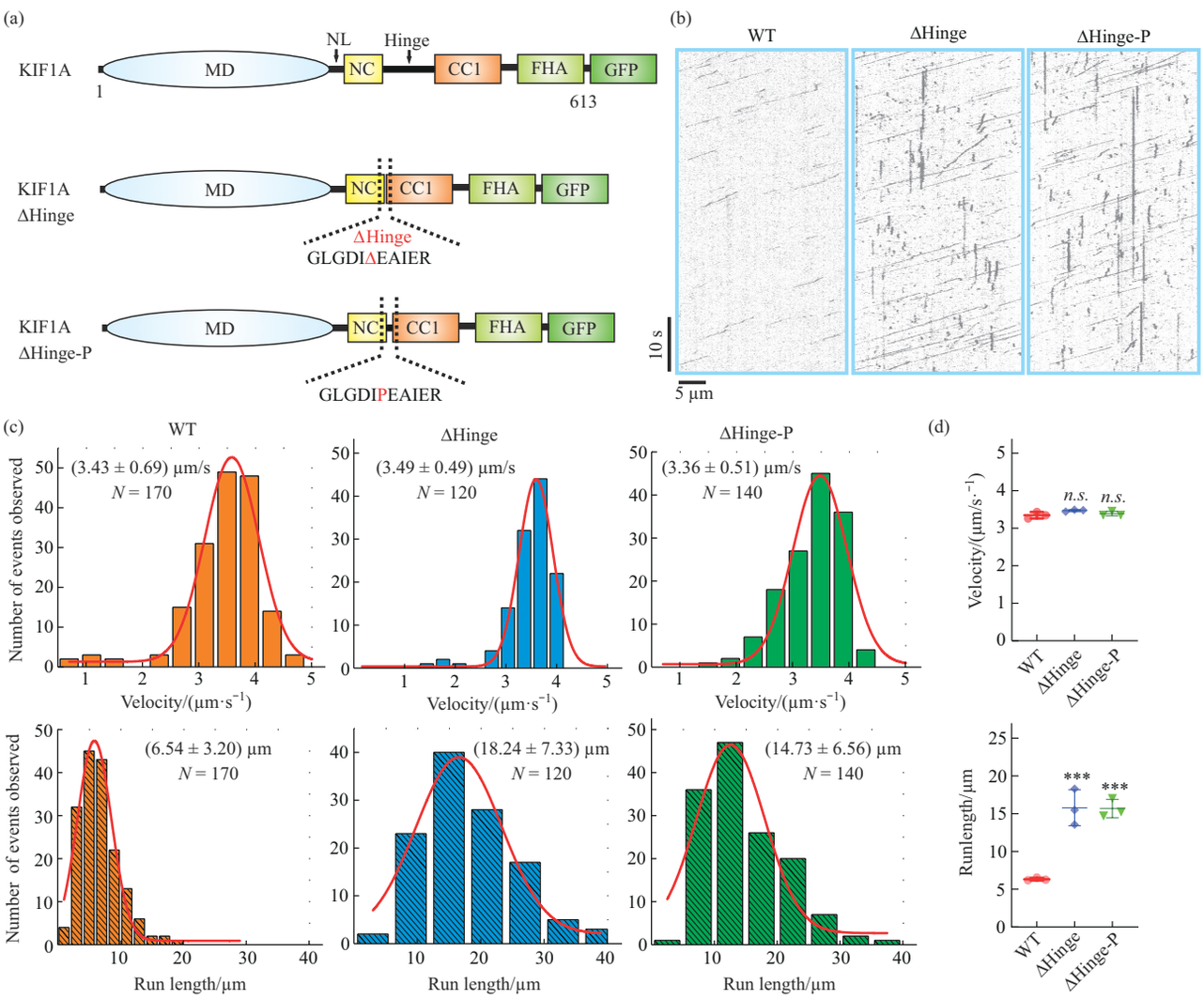

Fig. 2　Mutations of the flexible neck hinge impact the processivity of KIF1A

(a) Domain organizations of the MNCF fragment of KIF1A and its various mutants (ΔHinge and ΔHinge-P) used for the single molecule motility assay. (b) Representative kymographs showing the motions of the wild-type (WT) MNCF fragment of KIF1A and the ΔHinge and ΔHinge-P mutants along microtubules. (c) Quantifications of the velocity (top) and run length (bottom) for each protein sample. The number of events for each protein sample is plotted for the velocity and run length as a histogram and fitted to a Gaussian distribution. The velocity and run length of the corresponding population of the protein sample (*N*) are indicated in each panel as mean±SD. All the data are the average from at least two independent experiments. (d) Statistical analyses of the velocity (top) and run length (bottom) for each protein sample. Statistical significance for the velocity or run length is determined using Student's *t* test (*n.s.*, statistically not significant; ***P<0.001) as compared with the WT fragment of KIF1A.

In the wild-type protein, the processivity and velocity of KIF1A are both higher than that of KIF13B ((6.39±0.22) μm *v.s.* (2.76±0.43) μm, (3.37±0.09) μm/s *v. s.* (1.54±0.02) μm/s) (Figure 1c, 2c). Previous studies demonstrated that the motor domain of KIF1A possesses some intrinsic properties for the longer run length[14, 38], which may endow the capacity of KIF1A for the long-distance axonal transport of

synaptic vesicles in neurons. In this study, the deletion of the flexible neck hinge could further increase the processivity and generate an ultra-superprocessive motor (with run length of (16.44±2.53) μm) (Figure 2b−d), suggesting that the long flexible neck hinge has negative impacts on the processivity. We reasoned that the flexible neck hinge in KIF1A may be too long to disfavor the formation of the stable coiled-coil dimer in the extended neck and the deletion of this neck hinge could enhance the stability of the neck dimer (Figure S3b). On the other hand, the further insertion of the proline-hinge had no impact on the processive movement of KIF1A, possibly due to the variation of the C-terminal end of the NC. In KIF1A, the C-terminal end of the NC already contains the flexible residues (ended with Gly-Leu-Gly-Asp) that would likely buffer the restriction effect of the proline-hinge for processive movement (Figure S1b, S3b). Moreover, the intrinsic flexibility of the C-terminal end of the NC and the long neck hinge in the neck domain may also contribute to the higher motor speed of KIF1A (in comparison to KIF13B).

2.5 Switch of the mutated neck domain between KIF13B and KIF1A

In KIF13B and KIF1A, the neck hinge between the NC and CC1 in the NC-CC1-FHA tandem seems to break the extended neck to restrict processive movement and the removal of this neck hinge could increase the run length and/or speed (Figure 1, 2). To check whether the mutated neck domains of one motor has similar positive effects on the other, we next switched the hinge-truncated neck domain between KIF13B and KIF1A to generate the KIF13B-KIF1A ΔHinge and KIF1A-KIF13B ΔP391 chimeras (Figure S4a, e). In these two chimeras, the motor domain and neck linker were intact and the neck domain replacement was started from the NC (Figure S4a, e). Interestingly, in the KIF13B-KIF1A ΔHinge chimera, the KIF1AΔHinge neck could also significantly increase the run length and speed of KIF13B (from (2.76±0.43) μm to (6.27±0.18) μm and from (1.54±0.02) μm/s to (1.94±0.05) μm/s) (Figure S4b−d), similar to the positive effects induced by the ΔP391 mutation (Figure 1). In the KIF1A-KIF13BΔP391 chimera, the KIF13BΔP391 neck could significantly enhance the run length of KIF1A (from (6.39±0.22) μm to (13.09±0.26) μm) and moderately promoted the speed (from (3.37±0.09) μm/s to (3.62±0.08) μm/s) (Figure S4f−h), demonstrating the positive effects of the KIF13BΔP391 neck on KIF1A.

In these switch-based mutants of KIF13B and KIF1A, since the motor domain and neck linker were unchanged, the positive effects on the processivity and velocity would solely depend on the extended neck domain (Figure S4). In comparison to KIF13B with the ΔP391 mutation, the KIF1A-KIF13B ΔP391 chimera still exhibited a higher speed ((3.62±0.08) μm/s *v. s*. (2.21±0.01) μm/s) (Figure 1, S4), indicating that the N-terminal region of KIF1A including the motor domain and neck linker may possess the intrinsic capacity for the higher velocity in addition to the larger processivity. Moreover, in addition to the enhancement of the run length, the extra moderate increase of the motor speed induced by the KIF13B ΔP391 neck (with an extended coiled-coil) in the KIF1A-KIF13B ΔP391 chimera may also suggest that this dimeric neck could be the optimal neck of kinesin-3 for controlling processive movement. Taken together, the hinge-truncated neck domain could be switched between KIF13B and KIF1A to similarly tune their processive movement.

2.6 Engineering of the hinge−truncated neck domain of kinesin−3 into kinesin−1

To investigate the potential positive role of the mutated necks of kinesin-3 on other kinesin motors, we finally engineered the hinge-truncated neck domains of KIF1A and KIF13B into the conventional kinesin-1 to generate the KHC-KIF1A ΔHinge and KHC-KIF13B ΔP391 chimeras with the similar replacement strategy for the neck domain (Figure 3a). In these chimeras, the motor domain and neck linker of KHC were unchanged and attached to the KIF1A ΔHinge and KIF13B ΔP391 neck domains (Figure 3a). Interestingly, in comparison to the wild-type KHC, the replacements with the KIF1A ΔHinge and KIF13B ΔP391 neck domains both increased the run-length and speed of KHC (from (1.54±0.07) μm to (3.81±0.05) μm and (4.23±0.28) μm respectively, and from (0.87±0.01) μm/s to (1.24±0.01) μm/s and (1.08±0.06) μm/s respectively) (Figure 3b−d), suggesting that the hinge-truncated neck domains of KIF1A and KIF13B similarly boost the processive movement of kinesin-1. Thus, the hinge-truncated necks of kinesin-3 could be used by other processive kinesins to enhance the processivity and velocity.

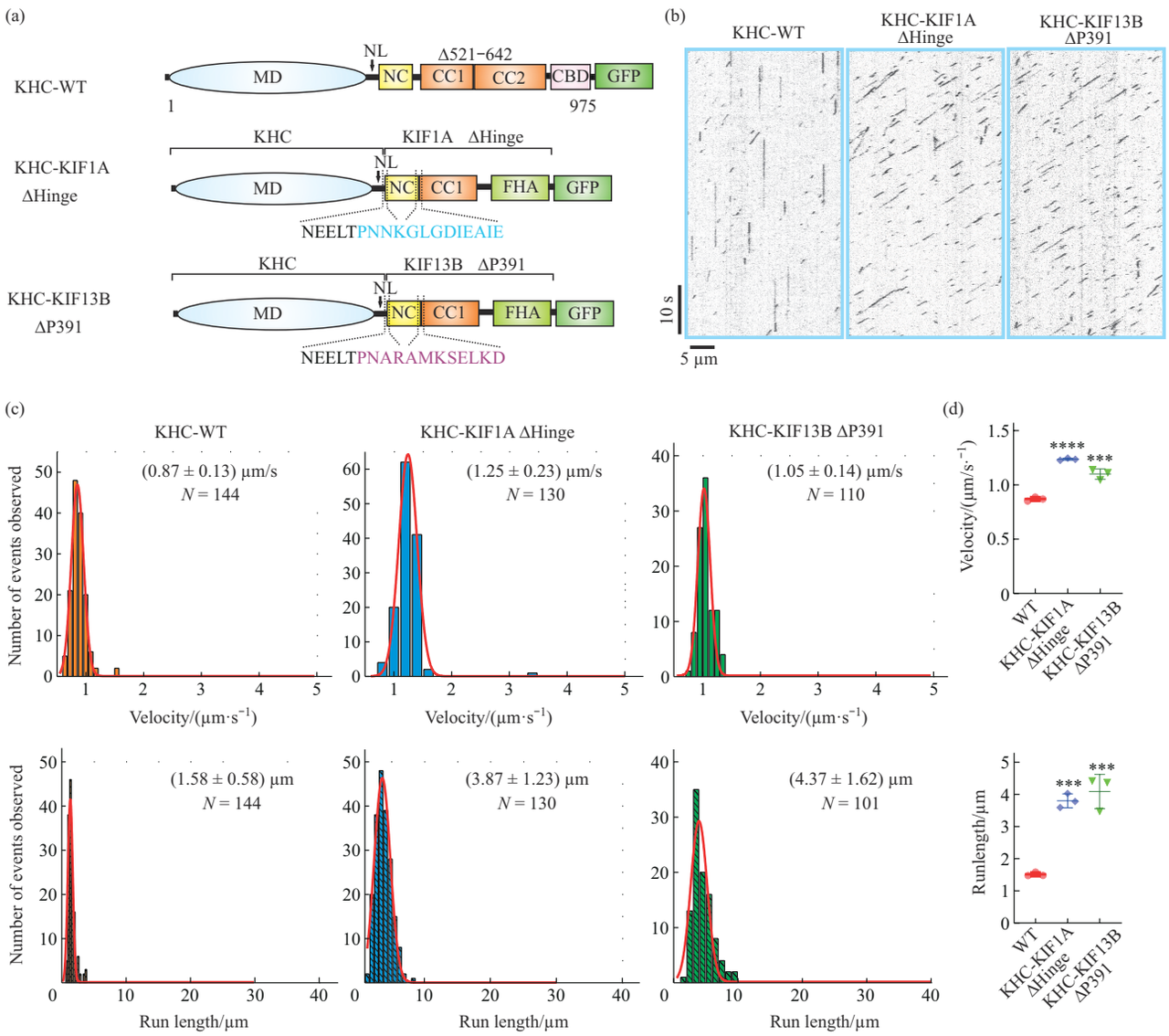

Fig. 3　Engineering of the hinge−truncated neck domain of kinesin−3 into kinesin−1

(a) Domain organizations of KHC (Δ521−642) and its various chimeras used for the single molecule motility assay. For the chimeras, the motor domain (MD-NL) of KHC is fused to KIF1A ΔHinge and KIF13B ΔP391 neck domains respectively. (b) Representative kymographs showing the motions of wild-type KHC (KHC-WT) and the KHC-KIF1A ΔHinge and KHC-KIF13B ΔP391 chimeras along microtubules. (c) Quantifications of the velocity (top) and run length (bottom) for each protein sample. The number of events for each protein sample is plotted for the velocity and run length as a histogram and fitted to a Gaussian distribution. The velocity and run length of the corresponding population of the protein sample (*N*) are indicated in each panel as mean±SD. All the data are the average from at least two independent experiments. (d) Statistical analyses of the velocity (top) and run length (bottom) for each protein sample. Statistical significance for the velocity or run length is determined using Student's *t* test (****P*<0.001, *****P*<0.000 1) as compared with KHC-WT.

3　Discussion

Kinesin-3 is a subfamily of kinesin motors for intracellular transport and contains different members[2, 4]. Based on the organization of the extended NC-CC1-FHA neck domain (Figure S1a, b), the neck hinge between the NC and CC1 is diverse in different kinesin-3 members but the precise role of this segment remains to be determined. In this study, we characterized the motor motilities of KIF13B and KIF1A with the various modifications of their neck hinges and uncovered the prominent role of the neck hinge for processive movement with a number of striking observations. Firstly, in KIF13B, the different modes of the proline-hinge breakage could differentially impact the processivity or velocity,

while the removal of the proline-hinge enhanced both (Figure 1). Secondly, in KIF1A, the deletion of the long flexible hinge significantly increased the processivity and tuned the motor to be an ultra-superprocessive one (with an average run length larger than 15 μm) (Figure 2). Thirdly, the switch of the mutated neck domain between KIF13B and KIF1A resulted in the similar enhancement in motor motilities (Figure S4), and the engineering of these hinge-truncated neck domains into kinesin-1 could also impact the processivity and velocity of kinesin-1 (Figure 3). All these striking observations demonstrate that the neck hinge controls the processive movement of kinesin-3 and the proper modulations of this characteristic segment can reshape the motor motility. Although the protein sequence alignment shows that the family members of kinesin-3 are relatively conserved in the NC-CC1-FHA region, further experiments are still needed to test whether the alteration of the neck hinge could impact the processivity in other kinesin motors.

In kinesin-3, due to the instability of the short NC coiled-coil dimer, the formation of the stable dimeric neck needs the CC1-FHA tandem that correlates with the preceding NC for controlling processive movement[18, 21]. The neck hinge between the NC and the CC1-FHA tandem seems to be essential for regulating the stability of the NC coiled-coil dimer and the flexibility of the entire extended neck (Figure S1a, b). Based on this study, a working model for the neck hinge-mediated regulation of the processive movement of kinesin-3 could be proposed (Figure 4). In this working model, in addition to the well-known determinants including the MD, NL, and NC, the neck hinge is an extra essential component for controlling motor motility (Figure 4). Due to the potential capacities of regulating the NC coiled-coil dimer and the flexibility of the neck domain, the neck hinge could function as a control center to modulate the run length and speed of the motor (Figure 4), resembling a gear lever for tuning processive movement. Consistent with this working model, the previous studies of kinesin-1 demonstrated that the flexible hinge immediately following the NC coiled-coil dimer (with the equivalent position of the neck hinge in kinesin-3) is also essential for controlling processive movement[13, 35].

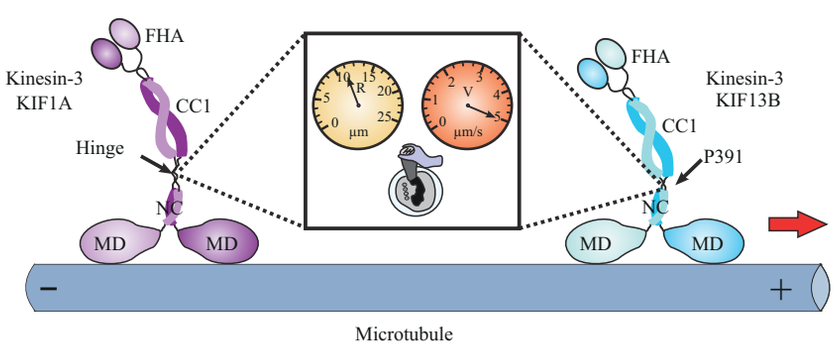

Fig. 4 A schematic model illustrating the neck hinge of kinesin−3 as a control center for tuning processive movement

In this schematic working model, in addition to the well-known determinants, the neck hinge of kinesin-3 is an extra essential component for controlling the motor motility. Due to the potential capacities of regulating the NC coiled-coil dimer and the flexibility of the neck domain, the neck hinge of kinesin-3 could function as a control center to modulate the run length and speed of the motor and thus resembles a gear lever for tuning processive movement.

4 Conclusion

In summary, the biochemical characterization of the processive movement of kinesin-3 demonstrated that the neck hinge could work as an additional control center for manipulating motor motility. The optimal extended neck of kinesin-3 could be engineered into other processive kinesins to enhance motor motility, which may pave the way for reshaping the processive movement of kinesin motors without touching the core determinants.

Supplementary Available online (http://www.pibb.ac.cn, http://www.cnki.net):
PIBB_20240269_Figure_S1.pdf
PIBB_20240269_Figure_S2.pdf
PIBB_20240269_Figure_S3.pdf
PIBB_20240269_Figure_S4.pdf

References

[1] Vale R D. The molecular motor toolbox for intracellular transport. Cell, 2003, **112**(4): 467-480

[2] Hirokawa N, Noda Y, Tanaka Y, *et al*. Kinesin superfamily motor proteins and intracellular transport. Nat Rev Mol Cell Biol, 2009, **10**(10): 682-696

[3] Cross R A, McAinsh A. Prime movers: the mechanochemistry of mitotic kinesins. Nat Rev Mol Cell Biol, 2014, **15**(4): 257-271

[4] Verhey K J, Kaul N, Soppina V. Kinesin assembly and movement in cells. Annu Rev Biophys, 2011, **40**: 267-288

[5] Vale R D, Milligan R A. The way things move: looking under the hood of molecular motor proteins. Science, 2000, **288**(5463): 88-95

[6] Vale R D, Fletterick R J. The design plan of kinesin motors. Annu Rev Cell Dev Biol, 1997, **13**: 745-777

[7] Woehlke G, Schliwa M. Walking on two heads: the many talents of kinesin. Nat Rev Mol Cell Biol, 2000, **1**(1): 50-58

[8] Endow S A. Determinants of molecular motor directionality. Nat Cell Biol, 1999, **1**(6): E163-E167

[9] Gennerich A, Vale R D. Walking the walk: how kinesin and dynein coordinate their steps. Curr Opin Cell Biol, 2009, **21**(1): 59-67

[10] Yildiz A, Tomishige M, Gennerich A, *et al*. Intramolecular strain coordinates kinesin stepping behavior along microtubules. Cell, 2008, **134**(6): 1030-1041

[11] Shastry S, Hancock W O. Interhead tension determines processivity across diverse N-terminal kinesins. Proc Natl Acad Sci USA, 2011, **108**(39): 16253-16258

[12] Thorn K S, Ubersax J A, Vale R D. Engineering the processive run length of the kinesin motor. J Cell Biol, 2000, **151**(5): 1093-1100

[13] Romberg L, Pierce D W, Vale R D. Role of the kinesin neck region in processive microtubule-based motility. J Cell Biol, 1998, **140**(6): 1407-1416

[14] Soppina V, Norris S R, Dizaji A S, *et al*. Dimerization of mammalian kinesin-3 motors results in superprocessive motion. Proc Natl Acad Sci USA, 2014, **111**(15): 5562-5567

[15] Wang W, Ren J, Song W, *et al*. The architecture of kinesin-3 KLP-6 reveals a multilevel-lockdown mechanism for autoinhibition. Nat Commun, 2022, **13**(1): 4281

[16] Hummel J J A, Hoogenraad C C. Specific KIF1A-adaptor interactions control selective cargo recognition. J Cell Biol, 2021, **220**(10): e202105011

[17] Fan X, McKenney R J. Control of motor landing and processivity by the CAP-Gly domain in the KIF13B tail. Nat Commun, 2023, **14**(1): 4715

[18] Huo L, Yue Y, Ren J, *et al*. The CC1-FHA tandem as a central hub for controlling the dimerization and activation of kinesin-3 KIF1A. Structure, 2012, **20**(9): 1550-1561

[19] Al-Bassam J, Cui Y, Klopfenstein D, *et al*. Distinct conformations of the kinesin Unc104 neck regulate a monomer to dimer motor transition. J Cell Biol, 2003, **163**(4): 743-753

[20] Ren J, Wang S, Chen H, *et al*. Coiled-coil 1-mediated fastening of the neck and motor domains for kinesin-3 autoinhibition. Proc Natl Acad Sci USA, 2018, **115**(51): E11933-E11942

[21] Ren J, Huo L, Wang W, *et al*. Structural correlation of the neck coil with the coiled-coil (CC1)-forkhead-associated (FHA) tandem for active kinesin-3 KIF13A. J Biol Chem, 2016, **291**(7): 3581-3594

[22] Gell C, Friel C T, Borgonovo B, *et al*. Purification of tubulin from porcine brain. Methods Mol Biol, 2011, **777**: 15-28

[23] Widlund P O, Podolski M, Reber S, *et al*. One-step purification of assembly-competent tubulin from diverse eukaryotic sources. Mol Biol Cell, 2012, **23**(22): 4393-4401

[24] Hyman A, Drechsel D, Kellogg D, *et al*. Preparation of modified tubulins. Methods Enzymol, 1991, **196**: 478-485

[25] Gell C, Bormuth V, Brouhard G J, *et al*. Microtubule dynamics reconstituted *in vitro* and imaged by single-molecule fluorescence microscopy. Methods Cell Biol, 2010, **95**: 221-245

[26] Schindelin J, Arganda-Carreras I, Frise E, *et al*. Fiji: an open-source platform for biological-image analysis. Nat Methods, 2012, **9**(7): 676-682

[27] Bornschlögl T, Woehlke G, Rief M. Single molecule mechanics of the kinesin neck. Proc Natl Acad Sci USA, 2009, **106**(17): 6992-6997

[28] Tomishige M, Klopfenstein D R, Vale R D. Conversion of Unc104/KIF1A kinesin into a processive motor after dimerization. Science, 2002, **297**(5590): 2263-2267

[29] Asbury C L, Fehr A N, Block S M. Kinesin moves by an asymmetric hand-over-hand mechanism. Science, 2003, **302**(5653): 2130-2134

[30] Yildiz A, Tomishige M, Vale R D, *et al*. Kinesin walks hand-over-hand. Science, 2004, **303**(5658): 676-678

[31] Rank K C, Rayment I. Functional asymmetry in kinesin and dynein dimers. Biol Cell, 2013, **105**(1): 1-13

[32] Gutiérrez-Medina B, Fehr A N, Block S M. Direct measurements of kinesin torsional properties reveal flexible domains and occasional stalk reversals during stepping. Proc Natl Acad Sci USA, 2009, **106**(40): 17007-17012

[33] Martin D S, Fathi R, Mitchison T J, *et al*. FRET measurements of kinesin neck orientation reveal a structural basis for processivity and asymmetry. Proc Natl Acad Sci USA, 2010, **107**(12): 5453-5458

[34] Ramaiya A, Roy B, Bugiel M, *et al*. Kinesin rotates unidirectionally and generates torque while walking on microtubules. Proc Natl Acad Sci USA, 2017, **114**(41): 10894-10899

[35] Grummt M, Woehlke G, Henningsen U, *et al*. Importance of a flexible hinge near the motor domain in kinesin-driven motility. EMBO J, 1998, **17**(19): 5536-5542

[36] Jaud J, Bathe F, Schliwa M, *et al*. Flexibility of the neck domain enhances Kinesin-1 motility under load. Biophys J, 2006, **91**(4): 1407-1412

[37] Crevenna A H, Madathil S, Cohen D N, *et al*. Secondary structure and compliance of a predicted flexible domain in kinesin-1 necessary for cooperation of motors. Biophys J, 2008, **95**(11): 5216-5227

[38] Scarabelli G, Soppina V, Yao X Q, *et al*. Mapping the processivity determinants of the kinesin-3 motor domain. Biophys J, 2015, **109**(8): 1537-1540

改造颈部铰链区重塑驱动蛋白3的持续运动能力*

李 冬[1,3)**] 任锦启[1)**] 宋银龙[2)] 梁 鑫[2)***] 冯 巍[1,3)***]

([1)] 中国科学院生物物理研究所，中国科学院生物大分子卓越中心，生物大分子国家重点实验室，中国科学院生物大分子重点实验室，北京 100101；

[2)] 清华大学生命科学学院，北京 100084；[3)] 中国科学院大学生命科学学院，北京 100049）

摘要 目的 驱动蛋白3的颈部螺旋与其后的蛋白质序列相互关联，形成一个延长的颈部，其中包含一个特征铰链结构。该特征性铰链在不同的驱动蛋白中表现出多样性，在驱动蛋白KIF13B中，这个铰链仅由一个脯氨酸残基组成，而在驱动蛋白KIF1A中，则由一个长的柔性无规卷曲构成。然而，这个颈部铰链在控制驱动蛋白持续运动方面的功能仍不明确。**方法** 本文对KIF13B和KIF1A的颈部铰链区的氨基酸残基进行突变改造，并通过单分子运动实验研究铰链区突变对驱动蛋白运动行为的影响。**结果** 在KIF13B中，在铰链区——脯氨酸前后插入柔性残基对其运动的速度以及持续性都有不同程度的影响，而去除该脯氨酸则可以同时提高运动速度和持续性。在KIF1A中，删除整个柔性颈部铰链仅仅增强了其运动的持续性。同时，把驱动蛋白1的颈部铰链区用改造后的驱动蛋白3的颈部铰链区进行替换，同样能够提高驱动蛋白1的持续运动能力。**结论** 驱动蛋白3颈部铰链控制其持续运动能力，适当改造可以调整马达的运动行为，这为重塑驱动蛋白马达的持续运动提供了一种新策略。

关键词 胞内物质转运，分子马达，驱动蛋白3，颈部铰链区，持续运动

中图分类号 Q51，Q71 **DOI**：10.16476/j.pibb.2024.0269

* 北京市自然科学基金（5242021），中国科学院战略性先导科技专项（XDB37020302），国家自然科学基金（32071191，32371273），科技创新2030-“脑科学与类脑研究”重大项目（2022ZD0205800）和中国科学院稳定支持基础研究领域青年团队计划（075）资助。

** 并列第一作者。

*** 通讯联系人。

梁鑫 Tel：010-62771231，E-mail：xinliang@mail.tsinghua.edu.cn

冯巍 Tel：010-64888751，E-mail：wfeng@ibp.ac.cn

收稿日期：2024-06-26，接受日期：2024-08-24